

- 225; J. Altman and G. D. Das, *J. Comp. Neurol.* **137**, 433 (1969).
10. C. M. Moorshead and D. van der Kooy, *J. Neurosci.* **12**, 249 (1992).
 11. S. Forss-Petter *et al.*, *Neuron* **5**, 187 (1990).
 12. SVZ and cortex were dissected from transgenic animals (10) and minced into ~100- μ m-diameter explants (7). Explants were suspended in Leibovitz L-15 medium plus glucose (6.5 mg/ml), and loaded into 100- μ m beveled glass pipettes. We grafted 200 nl of the explant suspension into the SVZ ($n = 4$) (1 mm anterior to bregma, 0.9 mm lateral, and 2.3 mm deep from the pial surface) or caudate nucleus ($n = 2$) (0.6 mm anterior to bregma, 1.5 mm lateral, 2.3 mm deep). After 30 days the brains were fixed, cut into 50- μ m-thick sections, and processed for X-gal histochemistry [M. G. Kaplitt *et al.*, *Molecular Cell. Neurosci.* **2**, 320 (1991)]. Both donors and hosts were males between 3 and 8 months old. Hosts were CB6/F₁ nontransgenic mice. When SVZ explants from CB6/F₁ nontransgenic animals were grafted into the SVZ of hosts ($n = 2$), X-gal⁺ cells were not detected in any region of the brain. Surgery was done under Nembutal (0.6 mg per gram of body weight) anesthesia.
 13. The X-gal⁺ cells in the graft site may have derived from two sources: (i) neurons from the striatum that surrounds the SVZ that survived after transplantation and (ii) neurons that differentiated from grafted SVZ cells.
 14. No X-gal⁺ cells were found between the olfactory bulb and the graft site. Migrating neural cells do not express NSE [P. J. Marangos and D. E. Schmechel, *Annu. Rev. Neurosci.* **10**, 269 (1987)].
 15. We microinjected 10 nl of [³H]T (NEN) (6.7 Ci/mmol, 1 mCi/ml) into the SVZ (1 mm anterior to bregma, 1 mm lateral, and 2.3 mm deep from the pial surface) of adult male CD-1 mice under anesthesia (2 to 8 months old). Animals were killed by a lethal dose of anesthetic 6 hours, 12 hours, 1 day, 2, 4, 6, and 15 days after [³H]T microinjection ($n = 2$ per group), perfused, and their brains cut in horizontal sections 6 μ m thick. Sections were processed for autoradiography (5) and counterstained with Hoechst 33258 (2.5 μ g/ml). The [³H]T-labeled cells were quantified with a computer-based mapping microscope [A. Alvarez-Buylla and D. S. Vicario, *J. Neurosci. Methods* **25**, 165 (1988)]. Fluoro-Gold was included (0.2%) with the [³H]T to mark the position of microinjections; at this concentration Fluoro-Gold did not label SVZ cells. For systemic injections (Fig. 3B), mice ($n = 3$) received a single intraperitoneal (IP) injection of 50 μ l of [³H]T. Animals were killed 6 hours later and processed for autoradiography.
 16. To calculate the rate of cell migration, we measured the distance between 10 leading [³H]T⁺ cells and the injection site with a computer-based microscope (15) at different survival times after [³H]T microinjection.
 17. N. A. O'Rourke, M. E. Dailey, S. J. Smith, S. K. McConnell, *Science* **258**, 299 (1992); G. Fishell, C. Mason, M. E. Hatten, *Nature* **362**, 636 (1993).
 18. H. J. Okano, D. W. Pfaff, R. B. Gibbs, *J. Neurosci.* **13**, 2930 (1993).
 19. The number of [³H]T-labeled cells and the number of autoradiographic grains per labeled cell were counted in three zones (Fig. 3): SVZ, olfactory bulb, and migratory pathway between the SVZ and the olfactory bulb. For each zone and survival time (two animals for each survival time), labeled cells were counted in 10 sections taken at different levels throughout each zone. The number of labeled cells counted in one animal ranged from 324 (15-days survival) to 1439 (6 hours survival). The total number of labeled cells was estimated from the average number of labeled cells per 6- μ m section multiplied by the number of sections that encompassed each region where labeled cells were found. Given the size range of labeled cell nuclei found in our material, it is not necessary to correct for cell splitting between 6- μ m sections [S. J. Clarck, J. Cynx, A. Alvarez-Buylla, B. O'Loughlin, F. Nottebohm, *J. Comp. Neurol.* **301**, 114 (1989)].
 20. Adult mice (under anesthesia) received stereotaxic microinjections of [³H]T (15) and a systemic IP injection of 100 μ l of BUdR (100 mg/ml, Sigma). Animals that received simultaneous injections ($n = 3$) of [³H]T and BUdR were killed 8 hours later. Animals that received injections 12 hours apart ($n = 3$) were killed 1 hour after BUdR injection. Polyethyleneglycol (PEG) sections were processed for BUdR immunocytochemistry [R. S. Nowakowski, S. B. Lewin, M. W. Miller, *J. Neurocytol.* **18**, 311 (1989)]. BUdR remains available to label dividing cells for less than 1 hour after systemic injection [D. S. Packard, R. A. Menzies, R. G. Skalko, *Differentiation* **1**, 397 (1973)].
 21. A 5% solution of Dil (10 nl) [DilC₁₈(3), Molecular Probes] dissolved in vegetable oil (Wesson) was stereotaxically injected into the SVZ of anesthetized adult mice (15). Six hours, 3 days, 6, 10, 15, and 30 days after Dil injection, animals ($n = 3$ per group) were killed, perfused with 3% paraformaldehyde in 0.1 M phosphate buffer, and their brains cut into 50- μ m-thick sections with a Vibratome. Sections were counterstained with Hoechst 33258 and wet-mounted with 80% glycerol plus 0.06% gelatin.
 22. M. E. Hatten and C. A. Mason, *Experientia* **46**, 907 (1990); P. Rakic, *ibid.*, p. 882; K. Kishi, *J. Comp. Neurol.* **258**, 112 (1987).
 23. A. I. Farbman, in *Cell Biology of Olfaction* (Cambridge Univ. Press, Cambridge, 1992), pp. 132–166.
 24. M. B. Luskin, *Neuron* **11**, 173 (1993).
 25. C. Walsh and C. L. Cepko, *Science* **255**, 434 (1992).
 26. All treatments on experimental animals were in accordance with institutional guidelines. We thank S. Forss-Petter and P. Danielson for the NSEp transgenic mice and F. Nottebohm, M. E. Hatten, and G. Fishell for comments on the manuscript. Supported by NIH grant NS 24478 and a Sinsheimer award to A.A.-B. C.L. is a recipient of a La Caixa Foundation graduate program fellowship.

3 December 1993; accepted 31 March 1994

Postsynaptic Induction and Presynaptic Expression of Hippocampal Long-Term Depression

Vadim Y. Bolshakov and Steven A. Siegelbaum

Long-term depression (LTD) is an activity-dependent decrease in synaptic efficacy that together with its counterpart, long-term potentiation, is thought to be an important cellular mechanism for learning and memory in the mammalian brain. The induction of LTD in hippocampal CA1 pyramidal neurons in neonatal rats is shown to depend on postsynaptic calcium ion entry through L-type voltage-gated calcium channels paired with the activation of metabotropic glutamate receptors. Although induced postsynaptically, LTD is due to a long-term decrease in transmitter release from presynaptic terminals. This suggests that LTD is likely to require the production of a retrograde messenger.

Long-term potentiation (LTP) in the hippocampus and neocortex (1) and LTD in the cerebellum (2) are two important examples of activity-dependent synaptic plasticity in the mammalian brain that is long-lasting. Both forms of synaptic plasticity are induced by an increase in the concentration of Ca²⁺ in the postsynaptic cell. However, the sources of Ca²⁺ are different. LTP in the CA1 region of the hippocampus requires Ca²⁺ influx through the N-methyl-D-aspartate (NMDA)-type glutamate receptors (1), whereas LTD in the cerebellum requires Ca²⁺ influx (3) through voltage-gated Ca²⁺ channels (4). The two forms of plasticity also differ in their sites of expression. LTD in the cerebellum results from a decrease in the postsynaptic response of Purkinje neurons to glutamate (2). LTP is thought to result from both enhanced presynaptic release of glutamate (1, 5, 6) in response to a retrograde messenger produced in the postsynaptic cell (7) and from an increased postsynaptic response (1, 6, 8).

Relatively little is known about hippocampal LTD in comparison to LTP (9).

Center for Neurobiology and Behavior, Department of Pharmacology, Howard Hughes Medical Institute, Columbia University, New York, NY 10032, USA.

However, the recent finding that prolonged, low-frequency (1 to 5 Hz) stimulation induces LTD (10–12) makes it possible to investigate the mechanism of induction and site of expression of hippocampal LTD. Although the induction of LTD in the hippocampus (10) and cerebral cortex (13) requires postsynaptic Ca²⁺ [see (14) for an opposing view], its source is less certain and may depend on influx through NMDA receptors (10, 11, 15), voltage-gated Ca²⁺ channels (16), or internal Ca²⁺ release after activation of metabotropic glutamate receptors (mGluRs) (13, 17). Moreover, it is not known whether hippocampal LTD is due to a decrease in transmitter release or to a decrease in the postsynaptic response to glutamate. Our study shows that hippocampal LTD resembles cerebellar LTD (4) because it requires the paired activation of mGluRs and postsynaptic Ca²⁺ entry through L-type voltage-gated Ca²⁺ channels. However, in contrast to the cerebellum, LTD in the hippocampus is expressed presynaptically and results from a long-lasting decrease in transmitter release.

LTD was studied without contamination from LTP in 3- to 7-day-old rats, a stage before the development of LTP (12), at the

synapse between CA3 and CA1 pyramidal neurons. Stimulation of the presynaptic Schaffer collateral pathway at 5 Hz for 3

min induced LTD of the excitatory postsynaptic current (EPSC) in CA1 neurons (Fig. 1, A and B) (18). LTD could be induced

only when we allowed the postsynaptic neuron to depolarize under current-clamp conditions during the 5-Hz stimulation and was blocked by voltage-clamping the CA1 neuron at -70 mV during stimulation. LTD occurs specifically in the stimulated pathway and thus is homosynaptic (10, 11, 18). LTD lasted at least 70 min with an average depression of the EPSC amplitude to $46.9 \pm 8.0\%$ of its control value.

The requirement for postsynaptic depolarization could reflect a role for a voltage-dependent postsynaptic Ca^{2+} influx. In support of this view, we find that LTD is blocked when 10 mM EGTA is included in the whole cell recording solution to buffer the internal Ca^{2+} concentration, $[\text{Ca}^{2+}]_i$, to concentrations below 10 nM (Fig. 1C), consistent with other findings (10, 13, 14). However, this high concentration of EGTA also reduces the normal resting $[\text{Ca}^{2+}]_i$ and blocks any increase in $[\text{Ca}^{2+}]_i$ in response to stimulation. To distinguish between a permissive role for resting Ca^{2+} versus an inductive role of a rise in $[\text{Ca}^{2+}]_i$, we used a pipette solution containing 11 mM BAPTA (1,2-bis-(*o*-aminophenoxy)ethane-*N,N,N',N'*-tetracetic acid), a rapid Ca^{2+} chelator, and 3 mM CaCl_2 to buffer $[\text{Ca}^{2+}]_i$ near its normal resting concentration of 100 nM. LTD was also blocked under these conditions, suggesting that an increase in $[\text{Ca}^{2+}]_i$ is required (Fig. 1D). However, increased $[\text{Ca}^{2+}]_i$ is apparently not sufficient to induce LTD because raising postsynaptic $[\text{Ca}^{2+}]_i$ through photolysis of the Ca^{2+} chelator DM-nitrophen did not alter the EPSC (Fig. 1E) (19).

Fig. 1. Dependence of LTD induction on postsynaptic depolarization and $[\text{Ca}^{2+}]_i$. **(A)** (Top) EPSCs recorded at -70 mV. (Bottom) We induced LTD by stimulating the Schaffer collateral pathway at 5 Hz for 3 to 4 min in current-clamp mode (arrow 2). The same stimulation was used during voltage-clamp conditions at -70 mV (arrow 1). The pipette contained a standard intracellular solution (0.4 mM Ca^{2+} and 1.1 mM EGTA). **(B)** Averaged data for LTD induced under current-clamp conditions (mean \pm 95% confidence interval; $n = 22$). $[\text{EGTA}]_i$ is the internal EGTA concentration. **(C)** Effect of 10 mM EGTA on induction of LTD ($n = 9$). Free pipette $[\text{Ca}^{2+}]$ was calculated to be <10 nM. **(D)** Block of LTD in cells with $[\text{Ca}^{2+}]_i$ buffered at 100 nM ($n = 6$). The pipette contained 11 mM BAPTA and 3 mM Ca^{2+} . In (B) through (D), LTD was induced (at arrows) with the same protocol as in (A) with arrow 2. **(E)** Cell loaded with 2 mM DM-nitrophen and 1.0 mM Ca^{2+} . Ultraviolet photolysis for 30 to 40 s (at arrow) caused no change in EPSC size ($n = 12$). Data in (C), (D), and (E) indicate the mean \pm SEM.

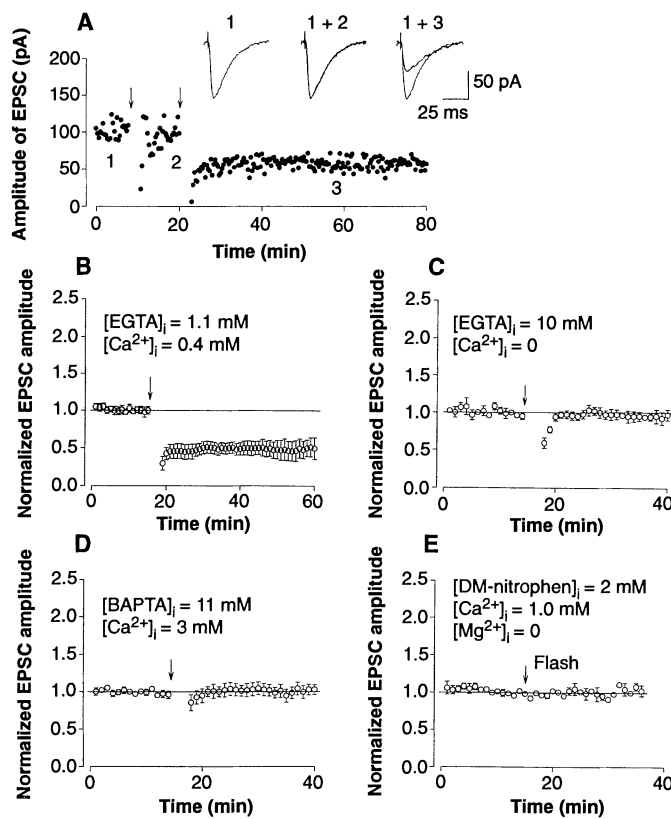
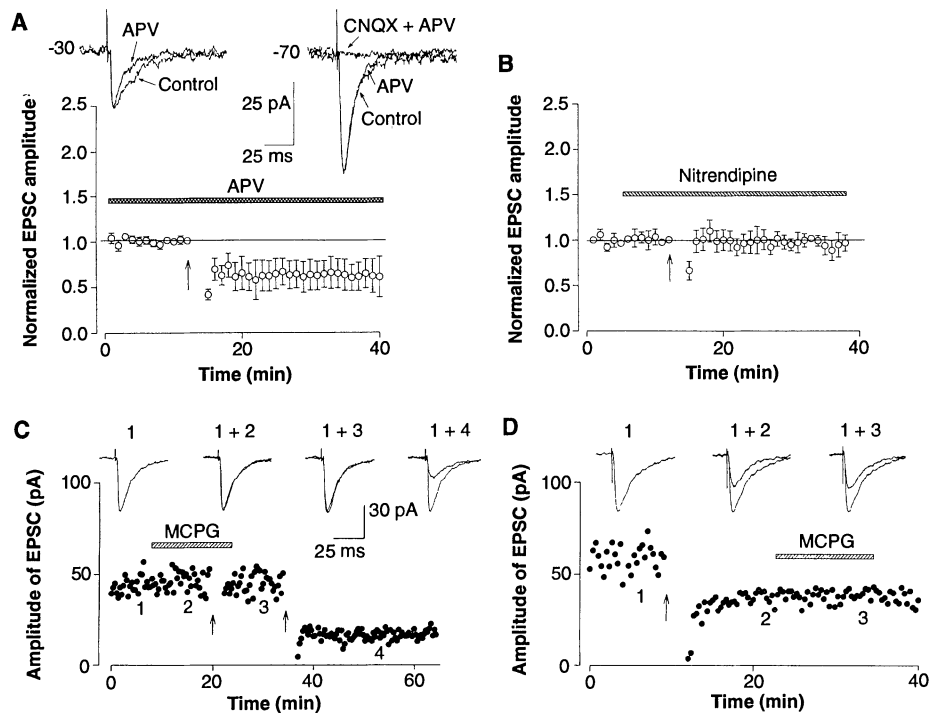


Fig. 2. Dependence of LTD induction on L-type Ca^{2+} channels and mGluR activation. **(A)** Block of NMDA receptors by *D*-APV did not block LTD. (Top) EPSCs recorded at holding potentials of -30 mV (left) or -70 mV (right). The *D*-APV (50 μM) blocked a slow component of the EPSC present at -30 mV but not at -70 mV. The EPSC was completely blocked by CNQX (20 μM), a selective blocker of non-NMDA glutamate receptors, and *D*-APV (50 μM). (Bottom) Graph shows average LTD in response to 5-Hz stimulation (arrow) in the presence of *D*-APV (EPSC reduced to $60.8 \pm 16\%$ of control; $n = 5$). The difference between the extent of LTD in the presence and absence of *D*-APV was not statistically significant (*t* test, $t = 1.013$). **(B)** Nitrendipine (5 μM ; Miles Pharmaceuticals, New Haven, Connecticut) blocked induction of LTD with 5-Hz stimulation (arrow) ($n = 5$). **(C)** MCPG (500 μM) blocked induction of LTD with 5-Hz stimulation (first arrow) ($n = 4$). After we washed away MCPG, 5-Hz stimulation induced LTD (second arrow). **(D)** MCPG (500 μM) did not block LTD when applied after LTD had been induced by 5-Hz stimulation (arrow). Labeled bars indicate periods of drug application; error bars indicate SEM.



What is the source of the increased $[Ca^{2+}]_i$? Induction of LTD was not blocked by the competitive NMDA receptor antag-

onist 2-amino-5-phosphonovaleric acid (D-APV) (Fig. 2A), although NMDA receptors are functionally expressed in the neo-

natal CA1 pyramidal neurons and contribute an APV-sensitive late component to the EPSC (Fig. 2A, top) (20). In contrast, nitrendipine, an inhibitor of L-type Ca^{2+} channels, blocked LTD induction (Fig. 2B). Nitrendipine did not alter basal synaptic transmission, suggesting that the L-type Ca^{2+} channels do not directly contribute to transmitter release.

Activation of mGluRs has been implicated in the induction of LTP (21) and LTD (13, 17). Thus, the fact that increased $[Ca^{2+}]_i$ caused by DM-nitrophen photolysis did not induce LTD could reflect a requirement for the paired activation of mGluRs. To test this idea, we used (*R,S*)-*a*-methyl-4-carboxyphenylglycine (MCPG), a selective mGluR antagonist (22) that blocks induction of hippocampal LTP (21). We found that in neonatal hippocampal neurons MCPG (500 μ M) selectively blocked mGluRs (Fig. 2C) (23). Moreover, MCPG blocked LTD induction in a fully reversible manner (Fig. 3C). The mGluR activation appears to be necessary for the induction but not the expression or maintenance of LTD because MCPG did not block LTD after it had been induced (Fig. 2D).

Is mGluR activation sufficient to induce LTD? Activation of mGluRs with the specific agonist *trans*-1-amino-cyclopentyl-1,3-dicarboxylate (ACPD) caused a reversible inhibition of synaptic transmission at the CA3-CA1 synapse (Fig. 3A) (24) that was blocked by MCPG (Fig. 3C) (25). The inhibition was presynaptic because ACPD produced no change in the amplitude of spontaneous EPSCs (sEPSCs) (Fig. 3B) (26). The reversibility of the inhibition

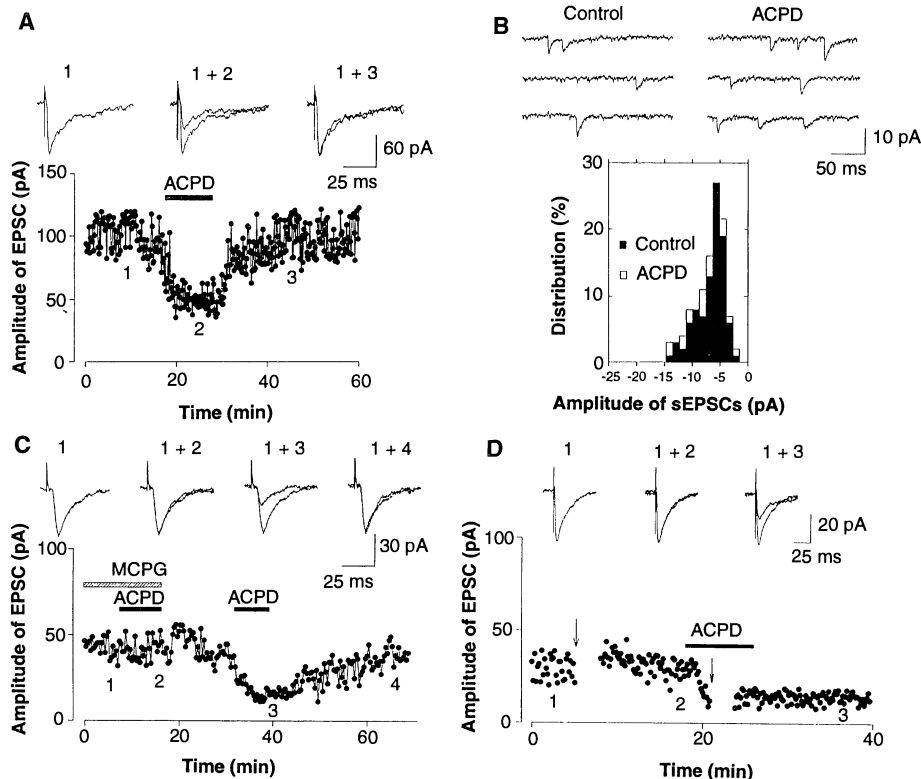
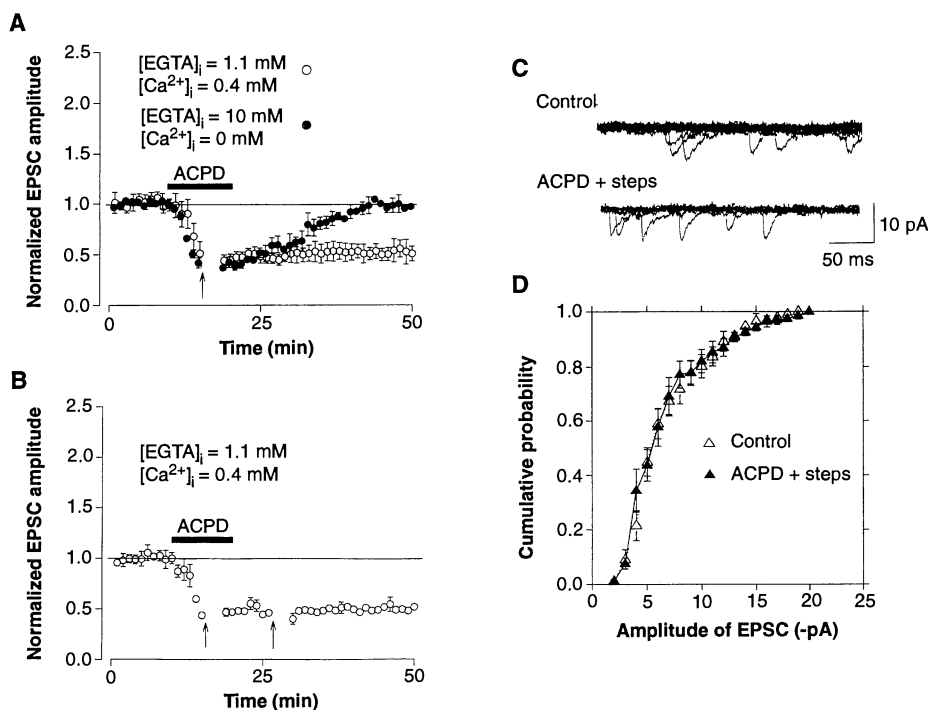


Fig. 3. Role of mGluRs in the induction of LTD. **(A)** Effect of ACPD (20 μ M) on EPSC (EPSC reversibly reduced to $47.2 \pm 2.4\%$ of control; $n = 21$). **(B)** ACPD (20 μ M) did not affect the amplitude distribution of sEPSCs (mean amplitude was -6.5 ± 0.24 pA, $n = 111$, before and -6.68 ± 0.26 pA, $n = 217$, after ACPD application). **(C)** Effect of MCPG (500 μ M) on presynaptic inhibition by ACPD. **(D)** Pairing ACPD application with a train of depolarizing postsynaptic pulses (second arrow) produced LTD. The depolarizing train applied alone (first arrow) had no effect (27).

Fig. 4. Properties of LTD induced by paired application of ACPD and postsynaptic depolarization. **(A)** Summary graph showing $[Ca^{2+}]_i$ requirement. Open symbols, pipette solution contained 1.1 mM EGTA and 0.4 mM Ca^{2+} ($n = 7$); filled symbols, pipette solution contained 10 mM EGTA and 0 mM Ca^{2+} ($n = 4$). Arrow indicates application of a train of depolarizing steps. **(B)** LTD induced by ACPD plus a train of depolarizing pulses (first arrow) occludes LTD with 5-Hz stimulation for 3 min (second arrow; $n = 3$). **(C)** Presynaptic locus for LTD induced by ACPD plus postsynaptic depolarization. Traces show sEPSCs before (top) and after (bottom) induction of LTD. **(D)** Cumulative average amplitude histogram of sEPSCs before (open symbols) and after (filled symbols) induction of LTD. Data were obtained from experiments shown in (A) (open symbols) ($n = 7$). All experiments were done in the presence of 100 μ M picrotoxin. Error bars indicate SEM.



with ACPD suggests that mGluR activation alone is insufficient to induce LTD.

The induction of LTD appears to require the pairing of postsynaptic depolarization with activation of mGluRs. Thus, application of ACPD during a train of short, depolarizing pulses applied to the CA1 neuron induced a long-lasting irreversible decrease in the EPSC (Figs. 3D and 4) (27). Similar to LTD produced by the 5-Hz stimulation, the ACPD-induced LTD was blocked by inclusion of 10 mM EGTA in the pipette solution, implying a requirement for postsynaptic Ca^{2+} (Fig. 4A). Moreover, induction of LTD with ACPD occludes the depression normally seen with 5-Hz stimulation (Fig. 4B), suggesting that the two processes are closely related.

To determine whether the site of expression of hippocampal LTD is postsynaptic, as in the cerebellum (2), or has a presynaptic component, as occurs with hippocampal LTP (1, 5, 6), we used an approach that relies on variations in the size of the EPSC generated by successive stimuli, previously applied to LTP (5). If we assume that synaptic variability reflects probabilistic release, the parameter M^2/σ^2 (where M is the mean EPSC amplitude and σ^2 is the variance in EPSC amplitude) provides an index

of synaptic function that is independent of postsynaptic transmitter sensitivity but reflects changes in transmitter release [(5); see (28) for an opposing view]. As shown in Fig. 5, induction of LTD is accompanied by a large change in M^2/σ^2 , suggesting a presynaptic effect.

Independent evidence for a presynaptic locus for LTD was derived from an analysis of sEPSC amplitudes; these amplitudes should reflect postsynaptic receptor sensitivity to the transmitter. To ensure that LTD was likely to be induced at all synapses, we induced LTD by pairing ACPD with postsynaptic depolarization. Despite a 50% decrease in the size of the evoked EPSC, there was no change in the sEPSC amplitude (Fig. 4, C and D; amplitude was -7.1 ± 0.4 pA before and -7.0 ± 0.4 pA after LTD induction; $n = 7$).

These results show that LTD in neonatal CA1 pyramidal cells depends on postsynaptic depolarization, inducing Ca^{2+} entry through L-type channels, paired with activation of mGluRs. Our results with 3- to 7-day-old rats agree with findings implicating mGluRs in LTD in adult rat hippocampus (17) and visual cortex (13) and in the related process of depotentiation, in which a low-frequency train of action potentials

reverses LTP (29). Our results differ from findings in hippocampal slices from 14- to 22-day-old rats in which induction of LTD required activation of NMDA receptors (10, 11) but not L-type channels (10), differences that could be related to the ages of the animals.

Although the induction of LTD has an important postsynaptic component, the expression of LTD appears to be presynaptic. This observation implies that, similar to LTP (7), LTD requires production of a retrograde messenger, consistent with evidence that nitric oxide might mediate LTD in the hippocampus (30). The similarity of LTD to presynaptic inhibition with ACPD suggests that the mGluRs may be presynaptic. This localization could explain the synapse specificity of LTD; only inputs active during the induction of LTD would receive a retrograde signal that resulted from increased postsynaptic $[Ca^{2+}]$ along with presynaptic mGluR activation. A requirement for presynaptic mGluR activation could also explain why it is often necessary to pair retrograde messengers with presynaptic stimulation to produce long-lasting changes in synaptic strength (7).

REFERENCES AND NOTES

1. T. V. P. Bliss and G. L. Collingridge, *Nature* **361**, 31 (1993).
2. M. Ito, *Annu. Rev. Neurosci.* **12**, 85 (1989).
3. M. Sakurai, *Proc. Natl. Acad. Sci. U.S.A.* **87**, 3383 (1990).
4. H. Daniel, N. Hemart, D. Jaillard, F. Crepel, *Exp. Brain Res.* **90**, 327 (1992).
5. J. M. Bekkers and C. F. Stevens, *Nature* **346**, 724 (1990); R. Malinow and R. W. Tsien, *ibid.*, p. 177.
6. D. M. Kullman and R. A. Nicoll, *ibid.* **357**, 240 (1992); A. Larkman, T. Hannay, K. Stratford, J. Jack, *ibid.* **360**, 70 (1992).
7. J. H. Williams *et al.*, *ibid.* **341**, 739 (1989); G. A. Bohme *et al.*, *Eur. J. Pharmacol.* **199**, 379 (1991); E. M. Schuman and D. V. Madison, *Science* **254**, 1503 (1991); M. Zhuo, S. A. Small, E. R. Kandel, R. D. Hawkins, *ibid.* **260**, 1946 (1993); C. F. Stevens and Y. Wang, *Nature* **364**, 147 (1993).
8. T. Foster and B. L. McNaughton, *Hippocampus* **1**, 79 (1991); T. Manabe, P. Renner, R. A. Nicoll, *Nature* **355**, 50 (1992).
9. R. C. Malenka, *Proc. Natl. Acad. Sci. U.S.A.* **90**, 3121 (1993); B. R. Christie and W. C. Abraham, *Synapse* **10**, 1 (1992); A. Artola, S. Brocher, W. Singer, *Nature* **347**, 69 (1990); V. A. Aroniadou and T. J. Teyler, *Brain Res.* **562**, 136 (1991); P. K. Stanton and T. J. Sejnowski, *Nature* **339**, 215 (1989).
10. R. M. Mulkey and R. C. Malenka, *Neuron* **9**, 967 (1992).
11. S. M. Dudek and M. F. Bear, *Proc. Natl. Acad. Sci. U.S.A.* **89**, 4363 (1992).
12. _____, *J. Neurosci.* **13**, 2910 (1993).
13. N. Kato, *Proc. Natl. Acad. Sci. U.S.A.* **90**, 3650 (1993).
14. F. Kimura, T. Tsumoto, A. Nishigori, Y. Yoshimura, *NeuroReport* **1**, 65 (1990).
15. W. C. Abraham and J. R. Wickens, *Brain Res.* **546**, 336 (1991).
16. J. R. Wickens and W. C. Abraham, *Neurosci. Lett.* **130**, 128 (1991).
17. P. K. Stanton, S. Chatterji, T. J. Sejnowski, *ibid.* **127**, 61 (1991).
18. Hippocampal slices (150 to 200 μ m) were prepared from 3- to 7-day-old Sprague-Dawley rats with a vibratome and continuously superfused in

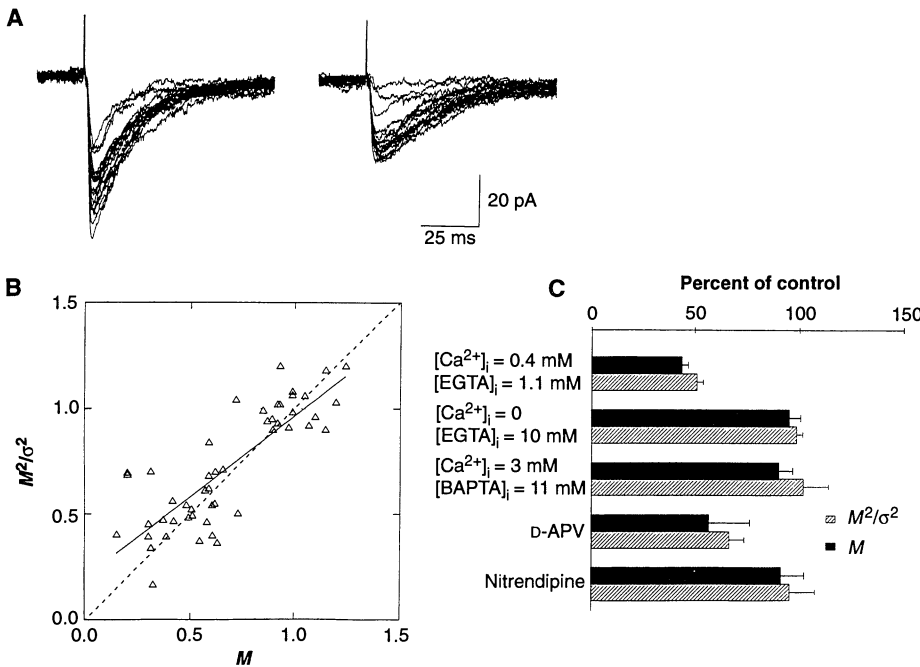


Fig. 5. Decreased transmitter release during LTD. **(A)** Variability in size of the EPSC elicited by successive stimuli before (left) and after (right) induction of LTD. **(B)** Effect of LTD induction on M^2/σ^2 versus M (solid line). Parameters were computed before and after 5-Hz stimulation. Each symbol is a separate experiment (150 to 400 trials analyzed in different experiments). Values of M^2/σ^2 and M measured during the period after stimulation were normalized by their values before stimulation. There is a correlation between changes in M and changes in M^2/σ^2 [r (correlation coefficient) = 0.82; $P < 0.05$]. The horizontal dotted line shows the predicted relation if LTD were purely postsynaptic. The dashed line shows the relation if the change in M^2/σ^2 is identical to the change in M . This occurs if LTD is presynaptic and due to either an increase in the number of release sites or an increase in the probability of release when this probability is low. **(C)** Summary of results from different protocols comparing changes in M and M^2/σ^2 .

artificial cerebrospinal fluid containing 119 mM NaCl, 2.5 mM KCl, 1.0 mM MgSO₄, 2.5 mM CaCl₂, 1.0 mM NaH₂PO₄, 26.2 mM NaHCO₃, and 10 mM glucose, equilibrated with 95% O₂ and 5% CO₂ (pH 7.3 to 7.4) at 21° to 23°C. In some experiments, picrotoxin (50 to 100 μM) was added to the bath solution with no effect on LTD (mean depression was 47.5 ± 10%, n = 10, in the absence of picrotoxin versus 45.5 ± 10%, n = 12, in the presence of 100 μM picrotoxin). Whole-cell patch-clamp recordings were obtained from CA1 pyramidal cells. The patch electrodes (5 to 10 megohms) contained 130 mM KCl, 0.4 mM CaCl₂, 1.1 mM EGTA, 1.0 mM MgCl₂, 5.0 mM NaCl, 10 mM potassium Hepes (pH 7.3), 2 mM Mg²⁺-adenosine triphosphate, and 0.1 mM Na⁺-guanosine triphosphate. Afferent fibers in the stratum radiatum were stimulated at 0.05 to 0.1 Hz with bipolar stainless steel electrodes. The holding potential was -70 mV. To elicit LTD, we applied a period of 5-Hz stimulation for 3 to 5 min under voltage-clamp or current-clamp conditions. Under current-clamp mode, the soma membrane depolarized by 15 to 25 mV during the train. We constructed summary graphs of EPSC amplitudes by normalizing data in 60-s epochs to the baseline EPSC recorded for 10 to 15 min at the start of each experiment. MCPG was purchased from Tocris Neuramin (Bristol, England), and DM-nitrophen from Calbiochem.

19. Ultraviolet (UV) illumination (Phillips 90-W quartz mercury high-pressure arc lamp), for 40 to 60 s in duration, was applied 15 min after obtaining the whole cell configuration. We estimated [Ca²⁺] to be > 1 μM, on the basis of microcuvette measurements with fura-2 (31). We omitted Mg²⁺ from the intracellular solution because of its high affinity for DM-nitrophen (32). Evidence that UV photolysis elevated [Ca²⁺] includes induction of a Ca-activated K⁺ current. Also, elevated [Ca²⁺] can participate in inducing LTD under appropriate conditions (27). Electrical stimulation of the Schaffer collaterals (3 min at 5 Hz) 5 to 8 min after photolysis of DM-nitrophen induced normal LTD (EPSC was reduced to 54.4 ± 2.8% of control; n = 3), indicating that the DM-nitrophen and UV light exposure did not inhibit LTD.
20. NMDA elicited inward currents (>100 pA) with typical voltage-dependent rectification. The D-APV (50 μM) decreased a late phase of the EPSC by 19 ± 5% at 25 ms (mean ± SEM; t = 3.2, P < 0.02, paired t test; n = 6).
21. Z. I. Bashir *et al.*, *Nature* **363**, 347 (1993).
22. S. A. Eaton *et al.*, *Eur. J. Pharmacol.* **244**, 195 (1993).
23. MCPG (500 μM) had no effect on the normal EPSC (Fig. 2C) or on NMDA-induced current.
24. A. Baskys and R. C. Malenka, *J. Physiol.* **444**, 687 (1991).
25. C. H. Davies *et al.*, *Soc. Neurosci. Abstr.* **19**, 276 (1993).
26. The sEPSCs were recorded on videotape for off-line analysis. Data were analyzed with the SCAN 4.0b program (J. Dempster, Dagan, Minneapolis, MN). Signals were compared with a threshold set above baseline noise (-1.5 to -2 pA), and samples were collected and stored when the threshold was exceeded. Noise artifacts and overlapping events have been excluded.
27. A train of short (50-ms) depolarizing steps to 0 mV at 5 Hz was applied to the postsynaptic neuron during ACPD application. This caused an irreversible presynaptic inhibition in all slices even after ACPD was washed out for 30 min (n = 7). The same train in the absence of ACPD had no effect on EPSC (n = 3). We also produced an irreversible depression of the EPSC by pairing ACPD with UV photolysis of DM-nitrophen (V. Y. Bolshakov and S. A. Siegelbaum, unpublished data), consistent with a role for increased [Ca²⁺] and providing a positive control for the experiment of Fig. 1E.
28. F. Edwards, *Nature* **350**, 271 (1991); H. Korn and D. Faber, *Trends Neurosci.* **14**, 439 (1991); T. Manabe, D. J. A. Wyllie, D. J. Perkel, R. A. Nicoll, *J. Neurophysiol.* **70**, 1451 (1993).

29. Z. I. Bashir *et al.*, *Eur. J. Pharmacol.* **239**, 265 (1993).
30. Y. Izumi and C. F. Zorumski, *NeuroReport* **4**, 1131 (1993).
31. L. S. Elliot, E. R. Kandel, S. A. Siegelbaum, H. Blumenfeld, *Nature* **361**, 634 (1993).
32. M. Morad, N. W. Davies, J. H. Kaplan, H. D. Lux,

Science **241**, 842 (1988).

33. We thank E. R. Kandel, T. O'Dell, and R. D. Hawkins for their comments on the manuscript and L. Zablou for help with the DM-nitrophen experiments.

16 February 1994; accepted 4 April 1994

Linkage Analysis of *IL4* and Other Chromosome 5q31.1 Markers and Total Serum Immunoglobulin E Concentrations

David G. Marsh,* John D. Neely, Daniel R. Breazeale, Balam Ghosh, Linda R. Freidhoff, Eva Ehrlich-Kautzky, Carsten Schou, Guha Krishnaswamy, Terri H. Beaty

Sib-pair analysis of 170 individuals from 11 Amish families revealed evidence for linkage of five markers in chromosome 5q31.1 with a gene controlling total serum immunoglobulin E (IgE) concentration. No linkage was found between these markers and specific IgE antibody concentrations. Analysis of total IgE within a subset of 128 IgE antibody-negative sib pairs confirmed evidence for linkage to 5q31.1, especially to the interleukin-4 gene (*IL4*). A combination of segregation and maximum likelihood analyses provided further evidence for this linkage. These analyses suggest that *IL4* or a nearby gene in 5q31.1 regulates IgE production in a nonantigen-specific (noncognate) fashion.

The immunogenetic mechanisms underlying heightened IgE responsiveness seen in the atopic diseases may be divided into two types, antigen (Ag)-specific and non-Ag-specific (1). The former is strongly influenced by HLA-D-encoded, major histocompatibility complex class II genes (1, 2) and involves cognate T cell-B cell interaction. The latter, noncognate regulation of IgE, could involve primarily basophils, mast cells, and possibly other FcεRI⁺ cells, with supplemental involvement of T cells (3, 4).

T helper lymphocytes, types 1 and 2 (T_H1 and T_H2), play a crucial role in facilitating the immune response (5, 6). The expression of several diseases can depend on whether T_H1 or T_H2 lymphocytes predominate in response to an Ag challenge (7). The IgE antibody (Ab)-mediated atopic allergies provide a particularly good model for studying T_H2-associated diseases. The Ag-cognate interaction of B cells with T_H2 cells involves CD40-CD40L binding, B cell activation, and the release of IL-4 and IL-13 from the T_H2 cells. This process leads to Ig heavy chain class-switching to the ε isotype, resulting in specific IgE Ab

responses (6, 8, 9). It appears that IL-5 facilitates IL-4-induced class-switching (10). Interleukin-4 is crucial for the development and functioning of T_H2 cells (5, 6, 8, 11), including their ability to express IL-5, leading to eosinophilia (11). It has been shown that activated normal human basophils express and secrete IL-4, in a process that is facilitated by IL-3 (3). The basophils are able to interact with B cells through CD40-CD40L, leading to the production of IgE (3). This interaction is not Ag-driven and is, therefore, noncognate. The overall production of IgE by both cognate and noncognate pathways is reflected in the total serum IgE concentration, which can readily be measured as a quantitative trait.

Studies of twins have shown that total serum IgE concentration is largely determined by genetic factors (12). Family studies have favored recessive, dominant, or codominant models for a postulated major gene controlling total IgE (1, 13, 14), usually with a significant polygenic influence (involving multiple minor genes). Estimates of heritability of log[total IgE] from twin and family studies of Caucasoid subjects range from about 0.37 to 0.84 (12, 14). Several family studies have provided evidence against linkage between a major gene for total IgE and HLA in chromosome 6p21.3 [reviewed in (1)]; also, the existence of an "atopy gene" in chromosome 11q13 is disputed (15).

The gene *IL4* has emerged as a major candidate for IgE responsiveness and atopy,

D. G. Marsh, J. D. Neely, B. Ghosh, L. R. Freidhoff, E. Ehrlich-Kautzky, G. Krishnaswamy, Johns Hopkins Asthma and Allergy Center, School of Medicine, 5501 Hopkins Bayview Boulevard, Baltimore, MD 21224, USA.

D. R. Breazeale and T. H. Beaty, Department of Epidemiology, Johns Hopkins School of Hygiene, Baltimore, MD 21205, USA.

C. Schou, Allergologisk (ALK) Laboratorium A/S, Bøge Allée 10-12, DK-2970, Hørsholm, Denmark.

*To whom correspondence should be addressed.